BNL-96172-2011-JA

Field Quality of the First LARP Nb_3Sn 3.7 m-Long Quadrupole Model of LQ Series

G. V. Velev, G. Ambrosio, N. Andreev, M. Anerella, R. Bossert, S. Caspi, G. Chlachidze, J. DiMarco, J. Escallier, H. Felice, P. Ferracin, V. V. Kashikhin, M. J. Lamm, F. Nobrega, E. Prebys, G. L. Sabbi, J. Schmalzle, M. Tartaglia, P. Wanderer, and A. V. Zlobin

***Abstract*—The US-LHC accelerator research program (LARP) built and tested the first 3.7-m long Nb_3Sn quadrupole model of LQ series with a 90 mm bore diameter and a target field gradient of 200 T/m. The LQ series, developed in collaboration among FNAL, LBNL and BNL, is a scale up of the previously tested 1-m long technology quadrupoles of TQ series based on similar coils and two different mechanical structures (shell-based TQS and collar-based TQC), with a primary goal of demonstrating the Nb_3Sn accelerator magnet technology for the luminosity upgrade of LHC interaction regions. In this paper, we present the field quality measurements in the first 3.7-m long LQS01 model based on the modified TQS mechanical structure. The results are compared to the expectations from the magnet geometry and magnetic properties of coils and iron yoke. Moreover, we present a comparison between this magnet and the short models previously measured.**

***Index Terms*—Magnetic field measurement, super-conducting accelerator magnets.**

I. Introduction

OVER the past several years, a collaboration of FNAL, LBNL and BNL as part of the US-LHC accelerator upgrade program (LARP), has been performing a research program on Nb_3Sn superconducting quadrupoles. The main goal of this program is to demonstrate that these Nb_3Sn magnets are a viable alternative for the LHC high luminosity upgrade of the interaction region (IR) quadrupoles [1].

As a first step in this research program, several 1-m long Nb_3Sn technology quadrupole models (TQ) with 90-mm aperture and the same type coils assembled in different supporting structures have been built and tested. A detailed discussion of the measurements of the first four TQ magnets is presented in [2]. Two of them (TQS01-02) were built by LBNL [3], [4] and the other two (TQC01-02) were built by Fermilab [5]–[7].

As a next logical step, for the first time, a 3.7 m long Nb_3Sn quadrupole (LQS01) with a shell-based segmented mechanical structure was built. The LQS01 is based on the TQS structure with some modifications to allow the assembly of the segmented structure, bring the axial rods closer to the coils, and alignment features from the pads to the shell (Fig. 1). LQS01 quadrupole performed extremely well during the quench tests and two sets of magnetic field quality measurements were taken with two different coil pre-stresses. More information about the production and the quench performance is presented elsewhere [8], [9].

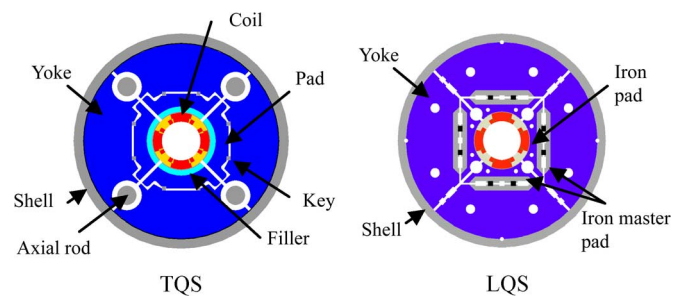

Fig. 1. Schematic view of the TQS and LQS yoked magnets.

In this paper, we present the results of magnetic measurements of the LQS01 magnet. Room temperature measurements were performed at yoked assembly prior to cooling down. They were followed by two sets of quality assurance magnetic measurements during cold testing of the magnet. It should be noted that neither the LQ nor the TQ models have alignment features during coil fabrication and assembly. These features have been introduced in the latest LARP magnet series (HQ) [10] that is therefore more representative of field quality in Nb_3Sn magnets.

II. Magnetic Field Measurements

All results in this paper are expressed in terms of harmonic coefficients defined in a series expansion given by

$$B_y + iB_x = B_2 10^{-4} \sum_{n=1}^{\infty} (b_n + ia_n) \left(\frac{x+iy}{r_0} \right)^{n-1} \quad (1)$$

where B_x and B_y in (1) are the field components in Cartesian coordinates, b_n and a_n are the 2n-pole normal and skew coefficients at the reference radius r_0 of 22.5 mm. This value was chosen as similar fraction of the official LHC reference radius of 17 mm to the IR quadrupole aperture of 70 mm. Probe centering is done using the standard technique of zeroing the dipole component assuming that it is purely generated from a probe offset in the quadrupole field. The right-handed measurement

Manuscript received August 02, 2010; accepted December 10, 2010. Date of publication January 28, 2011; date of current version May 27, 2011. This work was supported by the U.S. Department of Energy.

G. V. Velev, G. Ambrosio, N. Andreev, R. Bossert, G. Chlachidze, J. DiMarco, V. V. Kashikhin, M. J. Lamm, F. Nobrega, E. Prebys, M. Tartaglia, and A. V. Zlobin are with Fermi National Accelerator Laboratory, Batavia, IL 60510 USA (e-mail: velev@fnal.gov).

M. Anerella, J. Escallier, J. Schmalzle, and P. Wanderer are with the Brookhaven National Laboratory, Upton, NY 11973 USA.

S. Caspi, H. Felice, P. Ferracin, and G. I. Sabbi are with the Lawrence Berkeley National Laboratory, Berkeley, CA 94720 USA.

Color versions of one or more of the figures in this paper are available online at http://ieeexplore.ieee.org.

Digital Object Identifier 10.1109/TASC.2010.2100797

1051-8223/$26.00 © 2011 IEEE

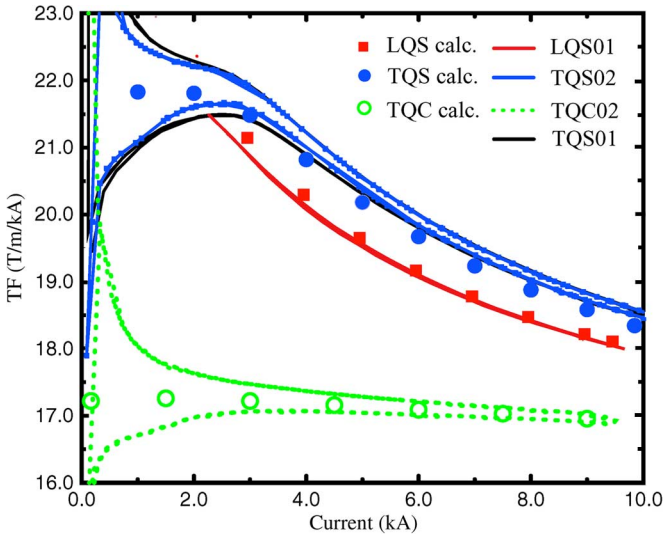

Fig. 2. Transfer functions for the magnets versus the excitation current. The filled (open) dots represent the calculations for TQS and TQC respectively. For comparison, the TQC02 TF is plotted too (dashed line).

TABLE I
CALCULATED AND MEASURED TQS AND LQS HARMONICS

b_n a_n	TQS calc.	TQS measured 01	TQS measured 02	LQS calc.	LQS measured
b_3	-	-1.46	2.98	-	3.43
b_4	-	-0.52	1.31	-	6.20
b_5	-	3.06	-1.45	-	-0.16
b_6	5.00	5.40	6.23	8.45	10.43
b_7	-	0.07	0.05	-	-0.10
b_8	-	-0.11	-0.13	-	-0.58
b_9	-	0.02	0.10	-	-0.14
b_{10}	0.04	0.02	-0.05	-0.03	-0.32
a_3	-	4.41	0.66	-	2.11
a_4	-	-1.99	0.82	-	1.34
a_5	-	0.71	-1.50	-	0.48
a_6	-	-0.37	0.12	-	-0.37
a_7	-	-0.11	-0.01	-	-0.30
a_8	-	-0.18	-0.10	-	-0.09
a_9	-	-0.02	0.02	-	-0.55
a_{10}	-	0.00	-0.08	-	0.24

TABLE II
TQ AND LQS HARMONICS AT 12.3 T/M, 100 T/M AND 200 T/M

b_n a_n	TQS01-02 average 12.3 T/m	TQS01-02 average 100 T/m	TQS01-02 average 200 T/m	LQS 12.3 T/m	LQS 100 T/m	LQS 200 T/m
b_3	0.73	0.01	0.06	3.34	2.29	2.61
b_4	-1.76	0.27	0.21	7.72	6.73	6.93
b_5	-0.88	1.57	0.39	0.06	0.17	-0.08
b_6	-11.83	3.83	1.58	-33.31	9.89	7.47
b_7	0.06	0.06	0.02	0.05	-0.06	-0.11
b_8	0.04	0.00	0.01	-0.28	-0.98	-0.38
b_9	0.03	0.02	0.00	0.08	0.19	0.13
b_{10}	0.12	0.03	0.00	0.56	0.35	-0.47
a_3	0.97	1.94	0.66	2.03	2.28	2.28
a_4	-3.70	-0.39	0.82	6.28	1.94	2.11
a_5	-0.24	0.30	-1.50	-0.50	-0.51	-0.65
a_6	0.13	-0.18	0.12	-1.14	-0.12	-0.29
a_7	-0.06	-0.09	-0.01	0.17	0.29	0.14
a_8	0.03	-0.10	-0.10	0.12	0.08	0.06
a_9	-0.01	-0.01	0.02	-0.29	-1.09	-0.16
a_{10}	0.00	-0.00	-0.08	0.05	0.37	0.12

coordinate system is defined with the z-axis at the center of the magnet aperture and pointing from return to lead end.

The magnetic measurements were performed at the Fermilab Vertical Magnet Test Facility (VMTF). Magnets were tested at 1.9 and 4.5 K; most of the measurements presented in the paper are taken at 4.5 K. For the test, we utilized two tangential-type rotating coil probes with a similar geometry and different lengths of approximately 0.1 and 0.8 m. TQ model magnets were measured with 0.1 m-length probe, while LQS measurements were performed with both probes.

A. *Transfer Function and Geometrical Harmonics*

The measured transfer functions (TF) in the magnets versus the excitation current is shown in Fig. 2. The loops are executed with ramp rate of 20 A/s. TQS and LQS, show a distinguishable similar pattern, which is determined from the iron characteristics. For example, one can see that TQS starts to saturate around 2.0–2.2 kA. For LQS we could not perform full loops because of the low ramp rate and low current conductor instability [11]. Moreover, we observed good agreement, below 0.2%, between the measured and calculated values. For comparison, we plot an example of the measured and calculated TF for a TQC-type model (TQC02E). Due to the collared coil structure in the magnets, the effect of saturations occurs much higher, after 7 kA (see Fig. 2, dashed line and open points).

Table I compares the average geometrical harmonics in the TQS and LQS magnets at 45 T/m (approximately 2.6 kA). At this gradient, the field penetrates fully in the superconductor and it is still below the iron saturation. Thus, we minimized the errors associated with these effects and possible imperfection in their simulation. Although achieving a particularly good field quality was not a TQS and LQS program target, one can see that harmonics differ from calculations [12] by less than ~6.2 units (normal octupole).

Table II compares the average harmonics measured at a current ramp up for LQS01 and TQS models at 12.3 T/m (LHC injection field), 100 T/m and at high current (~11 kA), close to the LHC IR quadrupole collision field. One may conclude that except for the octupole and dodecapole during the injection, which should be corrected for the next step in the program, LQS01 is practically an accelerator type quality magnet.

The reason for such octupole in LQS01 is most likely due to a deviation of the magnet aperture from circular to elliptical. The b_4 was not observed in the 1-m long TQS-TQC models. In LQS01 it may be generated during magnet assembly and/or by small differences in coil pairs fabricated with different fixtures (two sets of reaction and impregnation fixtures were used to make two LQ coils each, and coils made with the same set were placed facing each other during LQS01 and LQS01b assembly). This deviation will be addressed during next LQ assemblies.

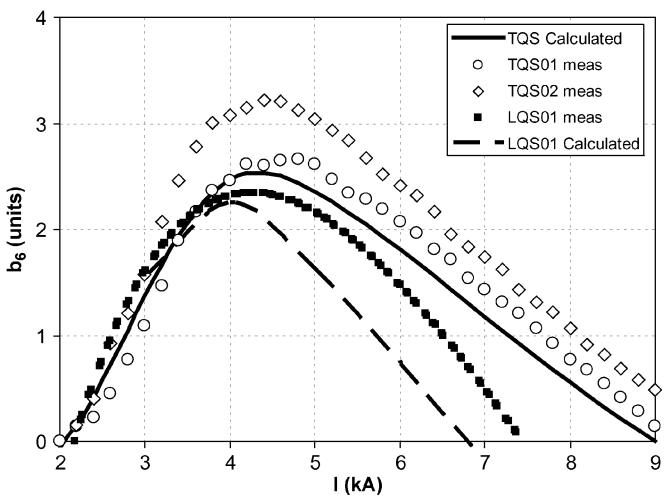

Fig. 3. Iron saturation effect in TQS01-02 and LQS01.

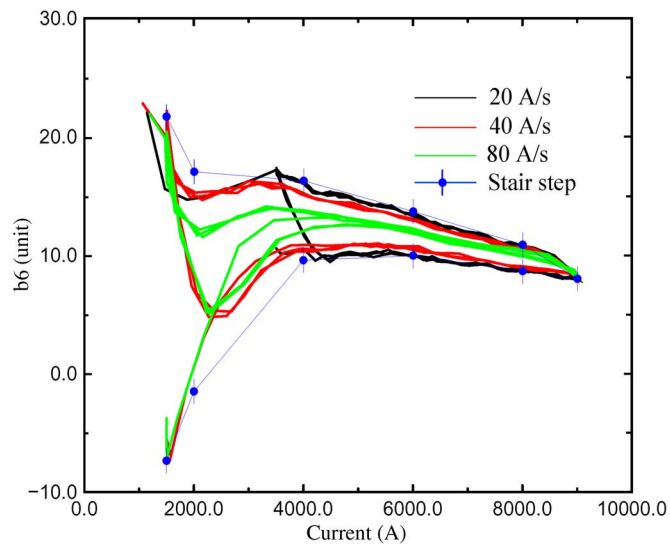

Fig. 4. LQS01 current loops executed at ramp rate of 20 A/s, 40 A/s and 80 A/s. The points represent the "stair step" measurement described in the text.

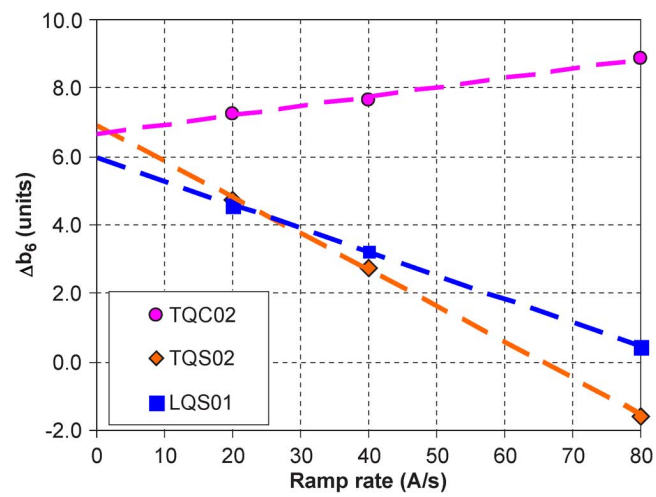

Fig. 5. Dodecapole loop width as function of the ramp rate.

B. Iron Saturation Effect

The iron saturation effect was extracted as an average value between up and down ramps of the measured hysteresis loops at 20 A/s and 40 A/s. The calculated and measured iron saturation effect in dodecapole for TQS and LQS magnets is shown in Fig. 3. One can see, that maximum observed dodecapole deviations are in the order of 2 units in LQS01 magnet and 3 units in TQS01-02 in current range from 2 kA to 9 kA. The larger iron saturation effect in these magnets is due to the iron pads placed next to the coil. As was discussed in [7], if it is necessary, the saturation effect can be corrected by introducing holes into appropriate places in iron pads and/or yoke, or by substituting the iron pads with stainless ones.

In comparison, the maximum dodecapole deviation due to the iron saturation in NbTi LHC IR magnets, which have the same iron yoke as TQC models, was approximately 0.2 units at the same fraction of the coil aperture.

C. Eddy Current Effect

Current excitation loops have been executed at current ramp rates of 20 A/s, 40 A/s, and 80 A/s for LQS01. Fig. 4 shows the measured dodecapole loops. The dots represent the "stair step" current profile measurement where the duration at every current step was set at 120 s. The measurements were started 5 s later after the current arrived at the plateau and the ramp rate between the steps was selected at level of 5 A/s. In this way, we minimized the possible eddy current effects to the measurement of the dodecapole hysteresis loop. Based on the presented results, one can conclude that LQS01 has relatively large interstrand coupling currents due to the low interstrand resistance. This problem can be solved by introducing a high resistivity core inside the cable.

The LQS01 and TQS02 (TQC02) magnets had coils of the same design made of the same RRP conductor with larger magnetization that should result in similar coil effects and dodecapole loop widths. Fig. 5 shows the widths of dodecapole $\Delta b_6 = (b_6^{\text{up ramp}} - b_6^{\text{down ramp}})$ loops at 90 T/m and different ramp rates. As expected, LQS01 and TQS02 show the same behavior, which is somewhat different from TQC02 dependence. This discrepancy could be attributed to the different coil structures. But for all of them, an extrapolation of Δb_6 to zero ramp rate is clearly similar and shows larger coil magnetization effect.

D. Long-Term Dynamic Effects

Long-term dynamic effects in superconducting magnets play an important role in the operation of modern accelerators. This well-known phenomenon is usually associated with the decay and subsequent snapback of the allowed field components at injection [13], [14].

To investigate these effects in the LQS01 quadrupole, we performed measurements with an accelerator current profile similar to the one used for the LHC IR quadrupole production tests, performed at Fermilab. The important characteristic of this profile is the duration of the injection plateau, which was set to ~900 s. Our measurements were focused on decay and snapback in the normal dodecapole component, the first allowed multipole.

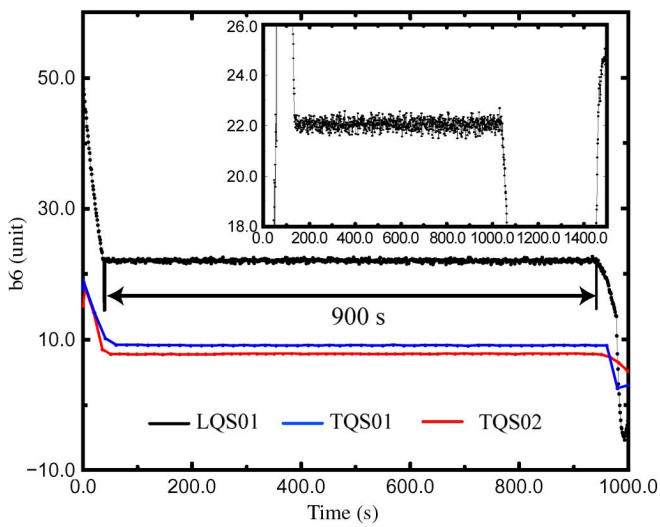

Fig. 6. Measurement of the decay and snapback of the dodecapole component for duration of injection of ~900 s in LQS and TQS magnets. No decay and snapback are observed.

As we expected, the decay and snapback was not observed in LQS01 (Fig. 6). The inset of Fig. 6 shows, in fine scale, the linearity of the dodecapole during the injection plateau. The LQS01 magnet behavior reproduces the results from TQ model quadrupoles [7]. The long-term decay and snap-back was not observed also in Nb_3Sn dipole model magnets made of similar conductors [15]. In comparison, average amplitude in the NbTi LHC IR quadrupoles was found to be 0.39 ± 0.11 [16]. Moreover, the long-term dynamic effects were not found in next allowed harmonics, b_{10}.

III. Summary

Magnetic field measurements were performed on the first 3.7-m long Nb_3Sn quadrupole model of LQ series with a 90 mm bore diameter. A comparison with the 1-m long TQS and in some cases with TQC, models was presented. The results show that the geometrical harmonics in LQS01, except for the normal octupole, are close to the requirements for accelerator type quality magnets. Additional work is required to improve the reproducibility of geometrical harmonics in Nb_3Sn quadrupoles [17]. This is among the goals of the HQ program [10].

The LQS01 eddy current effects were comparable with those observed in TQ magnets with coils made from the same type conductor. They are relatively large which is likely due to low interstrand contact resistances. If so, this effect can be reduced by using a stainless steel core inside the cable.

The long-term decay and snap-back effects were not observed in either of the Nb_3Sn TQ models or LQS01. This differs from the well-established results for NbTi IR quadrupole magnets, which demonstrated consistent decay and snap-back effect. However, it is consistent with the absence of snap-back in other Nb_3Sn magnets made of similar conductors. This phenomenon needs future investigation.

References

[1] S. A. Gourlay *et al.*, "Magnet R&D for the US LHC accelerator research program," *IEEE Trans. Appl. Supercond.*, vol. 16, no. 2, pp. 324–327, June 2006.

[2] G. V. Velev *et al.*, "Field quality measurements and analysis of the LARP technology quadrupole models," *IEEE Trans. Appl. Supercond.*, vol. 18, pp. 184–187, 2008.

[3] S. Caspi *et al.*, "Fabrication and test of TQS01-A 90 mm Nb_3Sn quadrupole magnet for LARP," *IEEE Trans. Appl. Supercond.*, vol. 17, pp. 1122–1125, 2007.

[4] S. Caspi *et al.*, "Test results of TQS02, a second Nb_3Sn quadrupole magnet model for LARP," *IEEE Trans. Appl. Supercond.*, vol. 18, pp. 179–183, 2008.

[5] S. Feher *et al.*, "Development and test of LARP technological quadrupole (TQC) magnet," *IEEE Trans. Appl. Supercond.*, vol. 17, pp. 1126–1129, 2007.

[6] Magnet TQC02 referenced in the text corresponds to the specific model TQC02Em.

[7] R. C. Bossert *et al.*, "Development and test of LARP technological quadrupole models of TQC series," *IEEE Trans. Appl. Supercond.*, vol. 18, pp. 175–178, 2008.

[8] P. Ferracin *et al.*, Mechanical Performance of the LARP Nb_3Sn Quadrupole Magnet LQS01, this conference.

[9] G. Ambrosio *et al.*, Test Results of the First 3.7 m Long Nb_3Sn Quadrupole by LARP and Future Plans, this conference.

[10] H. Felice *et al.*, "Design of HQ-A high field large bore quadrupole magnet for LARP," *IEEE Trans. Appl. Supercond.*, vol. 19, pp. 1235–1239, 2009.

[11] A. V. Zlobin *et al.*, "R&D of Nb_3Sn accelerator magnets at Fermilab," *IEEE Trans. Appl. Supercond.*, vol. 15, p. 1113, 2005.

[12] S. Russenschuck, *Field Computation for Accelerator Magnets*. New York: Wiley-VCH, 2010.

[13] D. A. Finley *et al.*, "Time dependent chromaticity changes in the Tevatron," in *Proc. 1987 PAC*, Washington, DC, 1987, pp. 151–153.

[14] G. V. Velev *et al.*, "Measurements of the persistent current decay and snapback effect in Tevatron dipole," *IEEE Trans. Appl. Supercond.*, vol. 17, pp. 1105–1108, 2007.

[15] V. V. Kashikhin *et al.*, "Field quality study in high-field Nb_3Sn accelerator magnets," in *Proc. of 2005 Particle Accelerator Conference*, Knoxville, TN, May 2005, pp. 366–338.

[16] G. V. Velev *et al.*, "Magnetic field measurements of LHC inner triplet quadrupoles fabricated at Fermilab," *IEEE Trans. Appl. Supercond.*, vol. 17, pp. 1109–1112, 2007.

[17] A. V. Zlobin *et al.*, " Nb_3Sn accelerator magnet technology R&D at Fermilab," in *Proc. of 2007 Particle Accelerator Conference*, Albuquerque, NM, June 2007, pp. 482–484.